Application of Computer Techniques in Correcting Mild Zygomatic Assymetry With Unilateral Reduction Malarplasty

Chong Zou, MD, Feng Niu, MD, Jian-feng Liu, MD, Bing Yu, MD, Ying Chen, MD, Meng Wang, and Lai Gui, MD

Abstract: Zygomatic assymetry is common in the population, which often requires surgical correction for aesthetic concerns. Previously, surgeons performed the surgery often based on their personal experience and visual evaluation. The purpose of this study was to apply computer techniques in patients with mild zygomatic asymmetry treated with unilateral reduction malarplasty to improve surgical accuracy and reduce preoperative risks. The authors used computer techniques to plan osteotomies, to produce surgical template, and to evaluate the surgical outcome. Postoperative follow-up demonstrated that zygomatic asymmetry was corrected in all the patients without complications. The proposed methodology was considered to be helpful in improving the surgical accuracy and efficiency for treatment of zygomatic asymmetry, while greatly minimizing operative risk.

Key Words: Computer techniques, L-shaped osteotomy, zygomatic asymmetry

Mild zygomatic assymetry with unilateral zygomatic prominence is common in the Chinese population. The pathology may be idiopathic, or as a presentation of hemifacial hyperplasia. For most of them, it is necessary to improve their facial appearance with surgery. As Asian women prefer a slender and oval face,[1] unilateral reduction malarplasty is often done on the larger side to restore facial symmetry.

Previously, surgeons performed the surgery based on their personal experience and visual evaluation, which often resulted in compromised surgical outcomes. The invisibility of zygomatic bone made surgical design and prediction more challenging. In recent years, with the development of digital technology, computer-assisted and rapid prototype manufacturing techniques have been used in craniofacial surgery. They have greatly improved the accuracy and surgical outcomes of craniofacial surgery.[2,3]

The purpose of this study was to apply computer techniques in 6 patients with mild zygomatic asymmetry treated with unilateral reduction malarplasty, and to develop a rational and effective treatment protocol.

From the Plastic Surgery Hospital, Chinese Academy of Medical Sciences and Peking Union, Medical College, Beijing, People's Republic of China.

Received February 6, 2015.
Accepted for publication March 1, 2015.

Address correspondence and reprint requests to Lai Gui, MD, The Craniofacial Center One, Plastic Surgery Hospital, Chinese Academy of Medical, Sciences, Peking Union Medical College, No. 33 Ba-Da-Chu Road, Shi-Jing-Shan District, 100144 Beijing, China;
E-mail: laiguiplastic@tom.com

The authors report no conflicts of interest.

Copyright © 2015 by Mutaz B. Habal, MD

ISSN: 1049-2275
DOI: 10.1097/SCS.0000000000001894

PATIENTS AND METHODS

From December 2012 to December 2014, 6 patients with mild zygomatic asymmetry who had undergone unilateral reduction malarplasty, assisted by computer techniques, were included in this study. Patients with congenital craniofacial anomalies, injuries, intellectual disability, syndromic conditions, and temporomandibular joint disorders were excluded from the study. This study was approved by the Peking Union Medical College's Ethical Committee. We obtained verbal informed consent from all subjects.

PREOPERATIVE PLANNING

A three-dimensional computed tomography (CT) examination (Brilliance CT 64 Slice, Philips Medical Systems, Cleveland OH) was performed before the surgery and half year after surgery. Axial scans were oriented parallel to the Frankfort horizontal plane. Analytic software Mimics 15.0 (Materalise, Leuven, Belgium) and Geomagic studio 12.0 (Geomagic, Morrisville, NC) was used for surgical planning and outcome analysis

Preoperative analysis was made from digitalized CT data. The image slice where the malar eminence appeared to be most prominent was selected for measurement. The malar eminence (P point) was marked on the most anterolateral aspect of the zygomatic complex. The midline (Y-axis line) was made by drawing the best fitting line from the vertical plate of the ethmoid to the midpoint of the spinosum foramina. A horizontal line perpendicular to the sagittal midline, when passing the posterior point of the zygomatic root, was defined as the X-axis line. The malar eminence was defined as the linear distance between P point to the origin point of coordinate axis. The DICOM files were used by the software to generate three-dimensional models of the skull. The images were reconstructed with a slice thickness of 1 mm. Three points (nasal spine, the midpoint of the sella turcica, and the internal occipital protuberance) were selected to define the sagittal plane for mirror imaging.

Three-dimensional models of the prominent side zygoma and the normal side were subtracted using a Boolean tool. The resulting subtraction image revealed the difference of malar prominence between the prominent and normal side (Fig. 1). We used these measurements as objective data to plan the extent of malar prominence to be reduced from the prominent side. An experienced senior surgeon determined the width and location of L-shaped osteotomy lines. A computer-aided surgery simulation was then performed on the three-dimensional skull (Fig. 2). Furthermore, the outcome of simulated surgery was checked and osteotomy lines were verified until desire surgical outcome was achieved. Then the individualized template was designed and made by using a rapid prototyping technique (Fig. 3A).

FIGURE 1. Mirror imaging and Boolean tool was used to determine the extent of malar prominence to be reduced from the prominent side.

FIGURE 2. A computer-aided surgery simulation was performed on the three-dimensional reconstructed skull model.

Copyright © 2015 Mutaz B. Habal, MD. Unauthorized reproduction of this article is prohibited.

FIGURE 3. A, The individualized surgical template was designed and made by CAD/CAM techniques. B, The individualized surgical template was used to guide intraoperative osteotomies. C, Titanium plates and screws were used for rigid fixation after osteotomies.

SURGICAL PROCEDURE

The operation was performed under general anesthesia. A labiobuccal vestibular incision was made down to the periosteum from the bilateral canine fossae to the first molars. Subperiosteal dissection was made on the anteroinferior part of the maxilla, the zygomatic body, and the anterior two-thirds of the zygomatic arch. An L-shaped osteotomy line was marked under the guidance of the template (Fig. 3B). After the L-shaped osteotomies were made, the bone fragment between 2 osteotomy lines were removed and a greenstick fracture was made at the root of the zygomatic arch from the inside by repetitive pressing and reciprocating movement of the zygomatic complex medially. Then, the mobilized zygomatic unit was displaced and rotated inwardly. Titanium plates and screws were used for rigid fixation on the zygomatic buttress across the vertical osteotomy lines. The bony step beside the osteotomy lines was burred until smooth (Fig. 3C).

POSTOPERATIVE EVALUATION

All patients underwent postoperative CT scans at 2 weeks after surgery. We performed the three-dimensional reconstruction on the basis of CT data and evaluated the postoperative results by comparing the preoperative design and postoperative three-dimensional images of the skull. Virtual images from preoperative design and postoperative three-dimensional images were registered and superimposed onto each other by using Geomagic studio 12. The differences of matching was calculated and displayed as rainbow chart to evaluate the surgical results.

RESULTS

The patients included 1 man and 5 women ranging in age from 19 to 42 years, including 4 idiopathic unilateral zygomatic prominence, and 2 hemifacial hyperplasia. Postoperative follow-up demonstrated that the zygomatic asymmetry was corrected in all the patients with mid-face shape greatly improved (Fig. 4). The reduction of malar eminence of the prominent side ranges from 3 to 6 mm. No major complications such as unexpected bone fractures or injury to the facial nerve occurred. All patients were satisfied with their facial appearance after surgery. Virtual images from preoperative design and postoperative three-dimensional images were registered and superimposed onto each other. The postoperative three-dimensional images found minimal differences with preoperative design (less than 2 mm) (Fig. 5).

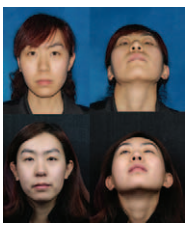

FIGURE 4. A 29-year-old woman with mild zygomatic assymetry. She had undergone unilateral reduction malarplasty on the right side. (Above) Preoperative frontal (left) and oblique views (right). (Below) Frontal (left) and oblique (right) preoperative "worm's-eye" views 1 year after surgery.

FIGURE 5. The comparison between simulated and postdistraction date by using rainbow chart; the green means the difference is less than 1 mm.

DISCUSSION

Mild zygomatic asymmetry with unilateral zygomatic prominence is common in the clinics, which often requires surgical correction for aesthetic and psychologic concerns. It may be clinical idiopathic zygomatic asymmetry, or as a presentation of hemifacial hyperplasia.[4,5] Previously, evaluation and surgical design was often done by visual measurement and personal experience. The surgery was often performed with poor precision, which often resulted in compromised surgical outcome.

In the 1990s, computer-aided design (CAD) and computer-aided manufacturing (CAM) techniques began to be used in craniomaxillofacial surgery and provided great advantages over conventional method in craniofacial reconstruction, craniosynostosis, macrocephaly, facial clefts, orthognathic surgery, and so on.[3,6–9]

In this study, we applied CAD and CAM techniques in the correction of mild zygomatic asymmetry with an L-shaped osteotomy. The proposed methodology could be easily and effectively applied to improve surgical accuracy and reduce operative risks. Firstly, preoperative measurement using mirroring techniques and Boolean tool could precisely determine the differences of malar prominence between affected and normal side. Secondly, preoperative surgery simulation allowed accurate design of the operative procedure on the basis of three-dimensional reconstructed model. With CAD/CAM techniques, the surgical templates were made to guide intraoperative osteotomies in accordance with preoperative design. It could greatly increase surgical efficiency and precision. Thus, the surgical time, blood loss, and overall surgical risks were reduced. What's more, the injury of maxillary sinus can be avoided to the greatest extent during surgical design and simulation. Finally, virtual images from preoperative design and postoperative three-dimensional images were superimposed onto each other and minimal differences were found. The rainbow chart gives a more intuitive approach to visualize the surgical outcomes and evaluate the feasibility of our method.

CONCLUSIONS

Computer techniques were applied in preoperative surgical design, surgical implementation, and postoperative evaluation in patients with mild zygomatic asymmetry treated with unilateral malar reduction. Our experiences indicate that good function and aesthetic outcomes with minimal operative risk could be achieved by using the proposed methodology.

REFERENCES

1. Gao ZW, Wang WG, Zeng G, et al. A modified reduction malarplasty utilizing 2 oblique osteotomies for prominent zygomatic body and arch. *J Craniofac Surg* 2013;24:812–817
2. Watson J, Hatamleh M, Alwahadni A, et al. Correction of facial and mandibular asymmetry using a computer aided design/computer aided manufacturing prefabricated titanium implant. *J Craniofac Surg* 2014;25:1099–1101
3. Seruya M, Borsuk DE, Khalifian S, et al. Computer-aided design and man-ufacturing in craniosynostosis surgery. *J Craniofac Surg* 2013;24:1100–1105
4. Hu J, Li Q, Zhang B, et al. Isolated hemifacial hyperplasia. *J Craniofac Surg* 2011;22:727–730
5. Sugiyama M, Tanaka E, Ogawa I, et al. Magnetic resonance imaging in hemifacial hyperplasia. *Dentomaxillofac Radiol* 2001;30: 235–238

© 2015 Mutaz B. Habal, MD

Copyright © 2015 Mutaz B. Habal, MD. Unauthorized reproduction of this article is prohibited.

6. Seruya M, Fisher M, Rodriguez ED. Computer-assisted versus conventional free fibula flap technique for craniofacial reconstruction: an outcomes comparison. *Plast Reconstr Surg* 2013;132:1219–1228
7. Wang J, Liu JF, Liu W, et al. Application of computer techniques in repair of oblique facial clefts with outer-table calvarial bone grafts. *J Craniofac Surg* 2013;24:957–960
8. Dorafshar A, Fisher M, Borsuk D, et al. A novel application of computer-aided design and manufacturing for reduction cranioplasty. *J Craniofac Surg* 2014;25:172–176
9. Swennen GR, Mollemans W, Schutyser F. Three-dimensional treatment planning of orthognathic surgery in the era of virtual imaging. *J Oral Maxillofac Surg* 2009;67:2080–2092

Simplified Designing and Insetting of the Free Flap in Reconstructing Oral and/or Oropharyngeal Defect

Jiyoung Yoon, MD, Ji Hong Yim, MD, and Eun Key Kim, PhD

Abstract: Reconstructing oral and/or oropharyngeal defect after tumor ablation requires anatomic restoration of the complex structures to maximize functional outcomes. This study introduces a simple and adjustable way of designing and insetting of a free flap in such reconstruction. Patients who received free flap reconstruction of oral and/or oropharyngeal defect with 33% to 66% of the native tongue left intact after resection of the tumor were enrolled and reviewed. Flap was designed as an oval shape according to the maximum width and length of the defect, and sutured from the most posterior part. Natural imbrication of the flap formed by anterior pulling of the tongue was marked and de-epithelized to create a three-dimensional shape. A total of 30 patients met the inclusion criteria of this study and the median follow-up was 32 months. All flaps survived after 1 case of venous reanastomosis. The average hospital stay was 23.7 days. All patients were decannulated. Twenty (66.7%) patients could eat a normal or soft diet, and 19 (63.3%) patients had normal or intelligible speech. Simplified designing of the flap with adjustable tailoring allowed for easy and effective way of free flap oral and/or oropharyngeal reconstruction. De-epithelization (or trimming) of the naturally imbricated area during the procedure of insetting created a bilobed shape in effect to conform to the three-dimensional defect.

Key Words: Free flap reconstruction, head and neck reconstruction, hemiglossectomy, oropharyngeal reconstruction

From the Asan Medical Center, University of Ulsan College of Medicine, Seoul, Korea.
Received December 21, 2014.
Accepted for publication March 22, 2015.
Address correspondence and reprint requests to Eun Key Kim, Asan Medical Center, University of Ulsan College of Medicine, 88, Olympic-Ro 43-Gil, Songpa-Gu, Seoul 138-736, Korea;
E-mail: nicekek@korea.com
The authors report no conflicts of interest.
Copyright © 2015 by Mutaz B. Habal, MD
ISSN: 1049-2275
DOI: 10.1097/SCS.0000000000001906

Reconstructing an oral and/or oropharyngeal defect after tumor ablation requires understanding of complex anatomic structures made up of multiple convex surfaces and sulci. Optimal reconstruction of the mobile tongue and mouth floor should aim to maintain the mobility of the remaining tongue by the use of a light, thin, and pliable flap when more than one third of the native tongue is left to preserve as much as possible its important functions including articulation, deglutition, and airway protection.[1] Because the efficacy and effectiveness of the microsurgical reconstruction for head and neck cancer patients have been established,[2–5] continued efforts will target anatomic classification of the defect and functional designing and insetting of the flap.[6–11] We propose here a simplified approach to designing and insetting of the flap for oral and/or oropharyngeal defect reconstruction after partial glossectomy, where the flap design is based on the maximum length and width of the flap, and the surfaces and sulcus are formed during insetting by de-epithelization or safe trimming of the distal part of the flap.

PATIENTS AND METHODS

Patients

This clinical study was conducted in accordance with the ethical guidelines of the authors' institution. Inclusion criteria for this study limited enrollment to adult patients with an oral/oropharyngeal defect with involvement of part of the tongue after resection of the tumor, having 33% to 66% of the native tongue left intact, and undergoing reconstruction with a free flap between January 2011 and April 2013.

Surgical Technique

The maximum length and width of the defect were measured with the tongue tip tagged and pulled forward. Maximum length was generally from the most posterior part of the defect to the tip of the tongue. Maximum width was calculated from the most lateral part of the defect to the dorsum of the tongue at the widest part of the defect, considering the curvature of the tongue and the floor of the mouth. Flap selection was based on the size of the defect and the thickness of the candidate donor sites. When the defect was small enough to be covered with a radial forearm free flap (RFFF), this method was our primary option. When the defect was more than approximately 12 cm in length or more than 8 cm in width, larger flaps such as an anterolateral thigh (ALT) free flap or a muscle-sparing rectus abdominis musculocutaneous (msRAM) free flap were considered. When the defect involved a part of the mandible, a fibular osteocutaneous (FOC) free flap was selected.

The flap was designed according to simple variables such as the maximum length and width of the defect (Fig. 1). Special attention was paid when the lateral pharyngeal wall or a substantial part of the tonsil was included in the defect because reconstruction of such regions usually required a separate lobe or additional width at the proximal-lateral aspect of the flap to avoid tethering. Flap

FIGURE 1. Design of a flap for hemitongue and the floor of mouth reconstruction. (Upper) Grossly oval shape was designed according to the maximum width and the maximum length of the defect. (Lower) Flap orientation and the approximate area to be de-epithelized.

© 2015 Mutaz B. Habal, MD

Copyright © 2015 Mutaz B. Habal, MD. Unauthorized reproduction of this article is prohibited.

FIGURE 2. Anterior pulling of the tongue during insetting. When insetting of the flap reached at the midway at the lateral direction, tongue tip was pulled together with the distal tip of the flap.

harvesting was similar in fashion with the previous reports, and the recipient vessels were chosen from the exposed vessels after neck dissection with matching caliber and reliable patency.

The flap was draped properly to form a neotongue surface and mouth floor. The suture started from the most posterior part of the defect (with the proximal aspect of the flap), continued bilaterally to meet the remaining tongue medially and margin of the mouth floor laterally. When addressing the widest part of the defect which was usually approximately midway, the distal tip of the flap was sutured to the tip of the remaining tongue and pulled forward to form the sulcus of the floor of the mouth (Fig. 2). This maneuver allowed spontaneous imbrication of the distal-lateral part of the flap at the site of the floor of the mouth (Fig. 3). The folded area was marked and de-epithelized using either a scalpel or scissors, or trimmed under direct visualization of the pedicle in case of a thick flap, and the skin flap had the shape of a bi-lobed skin paddle (Fig. 4). The margins of the de-epithelized (or trimmed) area were sutured together, and insetting continued to the tip of the tongue (Figs. 5 and 6).

Data Collection

The patients' demographics and oncologic status, defect location and size, flap of choice, and any surgical complications following surgical treatment were retrospectively reviewed. Functional evaluation was based on 2 numeric scales for speech (4—normal, 3—intelligible, 2—slurred, and 1—tracheostomy required) and swallowing (4—regular, 3—soft, 2—liquid, and 1—tube feeding dependent). Due to the descriptive nature of this study, no statistical analysis was performed.

RESULTS

After excluding patients who were lost to follow-up or had died, a total of 30 patients met the inclusion criteria for this study. The follow-up period ranged from 18 to 45 months with a median of 32 months. A total of 9 females and 21 males were included, and their mean age was 56.5-years old (range, 24–76 years). All but 2 patients were diagnosed with squamous cell carcinoma. All patients had a defect involving part of the tongue and the floor of the mouth: 18 patients had a tongue defect involving both the mobile and the basal part of their tongue; 10 patients had a tongue defect primarily involving the mobile part; 2 patients had a tongue defect was largely restricted to the base of the tongue, and the defect was extended to the tonsil in 6 patients (Table 1). The average length of the flap was 10.1 cm (range, 8–14 cm), and the average width of the flap was 6.7 cm (range, 5 to 10 cm) with an average dimension of 67.7 cm^2 (range, 35–100 cm^2). Twenty two RFFFs, 4 ALT free flaps, 3 msRAM free flaps, and an FOC free flap were used to cover the defects.

FIGURE 3. Flap draping and imbrication. Anterior pulling of the tongue tip caused natural imbrications of the flap at the floor of the mouth.

FIGURE 4. De-epithelization of the imbricated area. The area of natural folding was marked (upper) and de-epithelized (lower).

FIGURE 5. Immediate postoperative photograph. Hemitongue and the floor of the mouth was reconstructed with a radial forearm free flap.

FIGURE 6. Six months after reconstruction. This patient could eat regular diet, and had intelligible speech capability.

One venous thrombosis occurred but was salvaged through exploration and reanastomosis. Three cases of wound dehiscence were reported; 2 of which required wound repair. All flaps survived without significant sequel. The average hospital stay was 23.7 days, ranging from 16 to 42 days. Decannulation and tube feeding withdrawal were performed during the patient's hospital stay in most cases, but occasionally did occur in the outpatient clinic at follow-up. The average speech score was 2.80, and the average swallowing score was 2.93. Twenty (66.7%) patients could eat a normal or soft diet, and 19 (63.3%) patients had normal or intelligible speech. All patients were decannulated and independent of tube feeding. After 6 months postradiation patients were asked about any area of discomfort, and those issues were addressed. Three debulking procedures and 3 release procedures by Z-plasty were performed in the outpatient setting. All the debulking procedures were performed for the dorsum of the tongue, and all the release procedures were performed at the junction of the tongue, neotongue, or the floor of the mouth.

DISCUSSION

Advanced head and neck cancer is an important indication for free flap surgery, and the advantages of such reconstruction are well-established. Acceptable morbidities and quality of life following free flap reconstruction after radical ablation of oral/oropharyngeal cancer have been repeatedly evaluated,[2–5,12] and the merits of fasciocutaneous free flaps in certain indications are also well-known.[2,13] The goal of tongue reconstruction varies depending on how much of the native tongue is left intact. Although a total or subtotal glossectomy reconstruction requires sufficient bulk to prevent aspiration and to acquire acceptable speech function, a partial tongue reconstruction following hemiglossectomy demands a thin, pliable flap to maintain mobility of the remaining tongue.[1]

Several authors have published their method of designing and inserting a free flap to restore intraoral structures with a close three-dimensional resemblance to achieve optimal function and aesthetic outcome. The most direct way of approaching the issue is to anatomically classify the defect and to design a multilobed flap

© 2015 Mutaz B. Habal, MD

Copyright © 2015 Mutaz B. Habal, MD. Unauthorized reproduction of this article is prohibited.

TABLE 1. Patients' Oncologic and Surgical Data

Patient	Sex	Age	Indication	Stage	Location	Size, cm^2	Flap	Recipient Vessels	Adjuvant Therapy	Complication	Secondary Procedures
1	F	53	SqCC	T4aN1bM0	MT, FOM	9 × 6	RFFF	STA, STV, InnV	CT, RT	–	–
2	M	57	SqCC	T3N2cM0	MT, BOT, FOM, TO	13 × 7	ALT FF	FA, STV, InnV	CT, RT	–	–
3	M	26	Rhabdomyosarcoma	T3N0Mx	MT, BOT, FOM	10 × 8	ALT FF	FA, EJV	CT, RT	–	–
4	M	62	SqCC	T2N1cM0	MT, BOT, FOM	10 × 7	RFFF	STA, STV, IJV(s)	RT	–	–
5	M	72	SqCC	T4aN2bM0	MT, FOM	10 × 5	ALT FF	STA, IJV(s)	CT, RT	–	–
6	F	35	SqCC	T1N2cM0	MT, BOT, FOM	10 × 7	RFFF	STA, IJV(s)	CT, RT	–	–
7	M	62	SqCC	T4aN2cM0	MT, BOT, FOM	11 × 6	msRAM FF	FA, EJV	preCCRT	–	–
8	M	72	SqCC	T4aN2bM0	BOT, MT, FOM, RMT, MN	14 × 7	FOC FF	STA, EJV, IJV(s)	RT	–	–
9	F	55	SqCC	T4aN2bM0	MT, FOM	9 × 6	RFFF	STA, STV, EJV	CT, RT	–	Debulking
10	M	32	SqCC	T1N1M0	MT, FOM	9 × 5	RFFF	STA, EJV, IJV(s)	CT, RT	–	Release
11	F	76	SqCC	T4aN2bM0	MT, BOT, FOM, TO	12 × 6	RFFF	STA, STV, IJV(s)	preCCRT	–	–
12	M	57	SqCC	T4aN3M0	MT, BOT, FOM, TO	14 × 7	RFFF	STA, InnV, IJV(s)	CT, RT	–	–
13	M	75	SqCC	T2N2bM0	MT, BOT, FOM	11 × 7	RFFF	FA, EJV	preCCRT	–	–
14	M	61	SqCC	T1N1M0	MT, BOT, FOM	10 × 7	RFFF	STA, EJV, IJV(s)	preCCRT	–	Debulking
15	M	48	SqCC (recurrent)	rT1N0M0	MT, BOT, FOM	10 × 8	RFFF	FA, InnV, FV	CT	–	Release
16	F	24	SqCC	T4aN2bM0	MT, BOT, FOM, PW	11 × 8	RFFF	STA, IJV(s)	CT, RT	–	–
17	M	69	SqCC	T2N0M0	BOT, FOM, TO, PW	10 × 10	msRAM FF	STA, IJV(s)	CT, RT	–	–
18	F	47	Adenoid cystic carcinoma	T2N0M0	BOT, FOM, TO	10 × 7	RFFF	STA, IJV(s)	RT	–	–
19	F	50	SqCC	T2N0M0	MT, BOT, FOM	11 × 7	RFFF	STA, EJV, IJV(s)	RT	–	Release
20	M	62	SqCC	T1N0M0	MT, FOM	9 × 5	RFFF	STA, FV	preCCRT	–	–
21	M	55	SqCC	T4aN2bM0	MT, BOT, FOM	10 × 7	RFFF	STA, FV	RT	–	–
22	F	70	SqCC	T1N1M0	MT, FOM	8 × 6	RFFF	STA, STV, EJV	CT, RT	–	–
23	M	71	SqCC	T4aN2M0	MT, FOM	10 × 5	RFFF	STA, FV, EJV	CT, RT	Dehiscence	–
24	M	68	SqCC	T4aN1M0	MT, FOM	9 × 6	RFFF	STA, IJV(s)	CT, RT	–	–
25	M	69	SqCC (recurrent)	rT4N0M0	MT, BOT, FOM	10 × 7	RFFF	STA, FV	RT	–	–
26	F	56	SqCC	T4aN0M0	MT, FOM	7 × 5	RFFF	STA, STV, IJV(s)	CT	Dehiscence	Debulking
27	M	71	SqCC	T2N2cM0	MT, BOT, FOM	10 × 8	RFFF	STA, EJV, IJV(s)	CT, RT	Venous thrombosis, dehiscence	–
28	M	51	SqCC	T4aN2cM0	MT, FOM	8 × 6	ALT FF	STA, IJV(s)	CT, RT	–	–
29	M	48	SqCC	T2N2bM0	MT, BOT, FOM	11 × 8	RFFF	STA, FV, IJV(s)	RT	–	–
30	M	38	SqCC	T4aN2bM	MT (2/3), BOT, FOM	9 × 8	msRAM FF	FA, IJV(s)	CT, RT	–	–

ALT FF, anterolateral thigh free flap; BOT, base of tongue; CT, chemotherapy; EJV, external jugular vein; FA, facial artery; FOM, floor of mouth; FV, facial vein; IJV, internal jugular vein; InnV, innominate vein; MN, mandible; msRAM FF, muscle-sparing rectus abdominis musculocutaneous flap; MT, mobile tongue; preCCRT, preoperative concurrent chemoradiation therapy; PW, pharyngeal wall; RFFF, radial forearm free flap; RMT, retromolar trigone; RT, radiation therapy; SqCC, squamous cell carcinoma; STV, superior thyroid vein; TO, tonsil.

accordingly.[6,7] Although the details may vary, they also provide an excellent insight to the anatomy of the intraoral structures. A typical hemiglossectomy usually requires a bilobed flap, while repairs to the lateral wall require a separate lobe.[8] Hsiao et al[9] designed an asymmetrical bilobed flap and emphasized the need to form a narrow-waisted shape by applying some fixation sutures between the flap and the native tongue. Davison et al[10] made 2 modifications to the conventional flap design: first they rotate the native tongue tip to improve sensation, and they imbricate a de-epithelized wedge at the floor of the mouth to help anterior to posterior clearing. Our triangular de-epithelization or trimming resembles their design, but our purpose is different. Chepeha et al[11] approach the problem in more straightforward way, using a rectangular template to form the hemitongue and the floor of the mouth. Their method of measuring the dimensions of the flap is essentially similar to ours. The method of flap insetting of Chepeha et al[11] is described as "dynamic": segmentally proceeding from posterior, to dorsal, to anterior, and the tension caused by draping the flap forms the glossomandibular sulcus. In our current series, draping of the flap caused a triangular area of imbrication which is de-epithelized or trimmed to make a smooth three-dimensional shape (Figures 7 and 8). Our approach is easy to measure and open to adjustment during the time of insetting (Figures 9 and 10). De-epithelization or trimming occurs at the distal part of the flap with direct visualization of the pedicle.

It is difficult to compare the functional outcomes of different studies. Radiation obviously seems to have negative influence on the outcome of any reconstruction as Shin et al[14] have objectively shown; however, different fields, dosage, and methods of assessment make a direct comparison rather difficult. The extent of tumor invasion and surgical ablation along with other variables such as comorbidities or the tumor site have been known to affect the degree of postoperative function.[15,16] However, controversies still

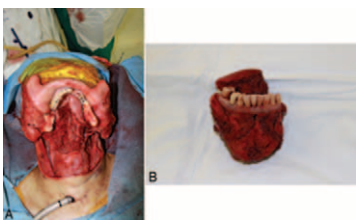

FIGURE 7. A case of a retromolar trigone cancer. (Left) Defect involved half of the tongue (mobile and base), the floor of the mouth, mandible with gingival, and the retromolar trigone after resection of the tumor (right).

© 2015 Mutaz B. Habal, MD

Copyright © 2015 Mutaz B. Habal, MD. Unauthorized reproduction of this article is prohibited.

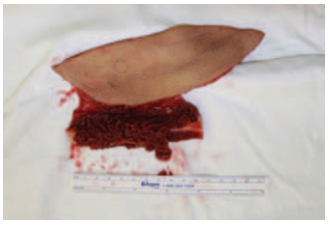

FIGURE 8. A fibular osteocutaneous flap. A fibular osteocutaneous free flap was harvested ($14 \times 7\,cm^2$).

FIGURE 9. Anterior pulling of the tongue. Natural imbrications were visible after the split lower lips were gathered.

FIGURE 10. After de-epithelization. Imbricated area was de-epithelized and sutured to form a three-dimensional shape.

exist whether the extent of resection of the soft palate, base of the tongue, or mobile tongue affects speech and/or swallowing functions.[4,15–17] Rieger et al[17] have reported that most patients, after reconstruction of the base of the tongue using RFFF, retain greater than 90% of speech intelligibility and normal oral feeding. Engel et al[1] demonstrated that 22 out of 33 patients had normal to intelligible speech, and 24 out of 33 patients could eat a normal or soft diet after a strategic tongue reconstruction after partial, subtotal, or total glossectomy. The data of Zafereo et al[5] show that after complex oropharyngeal reconstruction 86% of patients experience decannulation, 34% can fulfill their oral nutrition, and 69% have speech which is >80% intelligible. Approximately 67% of our patients could eat a normal or soft diet, and 63% attained normal to intelligible speech. None of the patients in our present series were feeding tube-dependent. Although it is difficult to compare our result with the previous studies, we believe the general outcome to be acceptable on a practical basis.

Even a sophisticatedly designed flap can subsequently become deformed pressure of the teeth or alveolus during the healing process can falsely mold the flap, and adjuvant radiation often results in unexpected deformation and shrinkage of the flap. Some authors suggest a 10% to 15% overcorrection occurs in case of expected radiation.[18] However, the effect of radiation on the flap volume or configuration appears to still be generally unpredictable, since some of our patients asked for flap debulking even after radiation. The junction of the native tongue, reconstructed neotongue, and the lower frenulum seemed to be the most vulnerable site to scar contracture. Tethering of this point often causes limited upward excursion of the tongue. Release and Z-plasty could be helpful in those cases.

In short, we suggest an alternative way of designing and insetting a free flap in an oral and/or oropharyngeal reconstruction, especially when a partial tongue and mouth floor is involved. A grossly oval flap is designed by measuring the longest and the widest dimensions of the defect, and then tacked from posterior to anterior. The triangular imbrication formed by draping the flap with the tip of the tongue extended is de-epithelized or trimmed to form a three-dimensional shape. This method is simple, adjustable, and safe to perform since the trimming can be done with direct visualization of the pedicle at the time of insetting.

REFERENCES

1. Engel H, Huang JJ, Lin CY, et al. A strategic approach for tongue reconstruction to achieve predictable and improved functional and aesthetic outcomes. *Plast Reconstr Surg* 2010;126:1967–1977
2. Guerin-Lebailly C, Mallet Y, Lambour V, et al. Functional and sensitive outcomes after tongue reconstruction: about a series of 30 patients. *Oral Oncol* 2012;48:272–277
3. Vega C, Leon X, Cervelli D, et al. Total or subtotal glossectomy with microsurgical reconstruction: functional and oncological results. *Microsurgery* 2011;31:517–523
4. Seikaly H, Rieger J, Wolfaardt J, et al. Functional outcomes after primary oropharyngeal cancer resection and reconstruction with the radial forearm free flap. *Laryngoscope* 2003;113:897–904
5. Zafereo ME, Weber RS, Lewin JS, et al. Complications and functional outcomes following complex oropharyngeal reconstruction. *Head Neck* 2010;32:1003–1011
6. Lew DH, Choi EC, Tark KC. Standardization of flap design for oropharyngeal reconstruction after cancer ablation surgery. *Yonsei Med J* 2003;44:1078–1082
7. Choi JW, Lee MY, Oh TS. The application of multilobed flap designs for anatomic and functional oropharyngeal reconstructions. *J Craniofac Surg* 2013;24:2091–2097
8. Yagi S, Kamei Y, Nakayama B, et al. A new design for free flap reconstruction of the tongue and oropharynx. *J Reconstr Microsurg* 2008;24:211–219
9. Hsiao HT, Leu YS, Lin CC. Tongue reconstruction with free radial forearm flap after hemiglossectomy: a functional assessment. *J Reconstr Microsurg* 2003;19:137–142
10. Davison SP, Grant NN, Schwarz KA, et al. Maximizing flap inset for tongue reconstruction. *Plast Reconstr Surg* 2008;121:1982–1985
11. Chepeha DB, Teknos TN, Shargorodsky J, et al. Rectangle tongue template for reconstruction of the hemiglossectomy defect. *Arch Otolaryngol Head Neck Surg* 2008;134:993–998
12. Bozec A, Poissonnet G, Chamorey E, et al. Quality of life after oral and oropharyngeal reconstruction with a radial forearm free flap: prospective study. *J Otolaryngol Head Neck Surg* 2009;38:401–408
13. Su WF, Hsia YJ, Chang YC, et al. Functional comparison after reconstruction with a radial forearm free flap or a pectoralis major flap for cancer of the tongue. *Otolaryngol Head Neck Surg* 2003;128:412–418
14. Shin YS, Koh YW, Kim SH, et al. Radiotherapy deteriorates postoperative functional outcome after partial glossectomy with free flap reconstruction. *J Oral Maxillofac Surg* 2012;70:216–220
15. Zuydam AC, Lowe D, Brown JS, et al. Predictors of speech and swallowing function following primary surgery for oral and oropharyngeal cancer. *Clin Otolaryngol* 2005;30:428–437
16. Bozec A, Poissonnet G, Chamorey E, et al. Radical ablative surgery and radial forearm free flap (RFFF) reconstruction for patients with oral or oropharyngeal cancer: postoperative outcomes and oncologic and functional results. *Acta Otolaryngol* 2009;129:681–687
17. Rieger JM, Zalmanowitz JG, Li SY, et al. Functional outcomes after surgical reconstruction of the base of tongue using the radial forearm free flap in patients with oropharyngeal carcinoma. *Head Neck* 2007;29:1024–1032
18. Haughey BH, Taylor SM, Fuller D. Fasciocutaneous flap reconstruction of the tongue and floor of mouth: outcomes and techniques. *Arch Otolaryngol Head Neck Surg* 2002;128:1388–1395

© 2015 Mutaz B. Habal, MD

Copyright © 2015 Mutaz B. Habal, MD. Unauthorized reproduction of this article is prohibited.

Cytotoxic Effects of Intranasal Midazolam on Nasal Mucosal Tissue

Isa Ozbay, MD,[*] Cuneyt Kucur, MD,[*]
Ayşenur Değer, MD,[†] Ilker Ital, MD,[‡]
Muhammet Kasim Cayci, PhD,[§] and Fatih Oghan, MD[*]

Abstract: The aim of this experimental study was to investigate the cytotoxic effects of intranasal midazolam on nasal mucosal tissue in rats. Forty healthy rats were randomly divided into 5 groups. Group 1 (n = 8) was the control group, group 2 (n = 8) received intranasal saline, group 3 (n = 8) received intranasal midazolam, group 4 (n = 8) received intraperitoneal saline, and group 5 received intraperitoneal midazolam (n = 8). Midazolam and saline were administered via intraperitoneal and intranasal routes at doses of 200 μg/kg. Nasal septal mucosal stripe tissues were removed at the 6th hour. All materials were evaluated according to Ki67 and p53 staining to evaluate proliferation and apoptosis, respectively, and hemotoxylin and eosin staining was performed for histopathology evaluation. Ki67 values and inflammation in group 3 were statistically higher compared to group 1, group 2, and group 4. P53 values in group 3 were statistically higher compared to group 1. Assessment of subepithelial edema between group 3 and the other groups revealed no statistically significant differences. Assessment of cilia loss between group 3 and group 1, group 2, and group 4 revealed no statistically significant difference. The evaluation of goblet cell loss between group 3 and group 1 revealed a statistically significant difference. Intranasal midazolam had adverse effects on nasal mucosa. However, intranasal midazolam is as safe as systemic midazolam administration with respect to nasal mucosa.

Key Words: Intranasal route, midazolam, proliferation, rats

Midazolam is a water soluble benzodiazepine that is directly absorbed by nasal mucosa and rapidly enters the blood and cerebrospinal fluid (CSF).[1] Drug absorption is affected by blood circulation in the nasal mucosa, the area of mucosa in contact with drug, and the drug concentration. The half-life of the drug is generally between 1.5 and 3.5 hours.[2] After application of 0.2 mg/kg intranasal midazolam, plasma levels reach 100 ng/mL in about 6 minutes.[3] Serum levels of intranasal midazolam are comparable with injectable levels after a few minutes of dispensation.[4] The intranasal route is preferable because it prevents the need for the intravenous route, it is easily applied, and permits a more rapid rate of absorption compared with the oral route.[5,6]

Ki67, a nuclear marker, is directly related to tumor cell proliferation. Ki67 has a positive correlation with prognosis in a diverse array of malignant tumors.[7,8] Functional p53 plays a significant role in preserving genomic constancy, orchestrating the cell cycle, and stimulating apoptosis.[9] As mutated p53 aggregates in the nucleus of tumor cells, immunohistochemical (IHC) staining for p53 is consistently used as a substitute marker for p53 mutational status.[10]

Information on the cytotoxicity and side effects of midazolam after intranasal administration is lacking in the literature. Therefore, herein we aimed to evaluate the cytotoxicity of intranasal midazolam on rat nasal mucosa, and to our knowledge, this is the first study evaluating the cytotoxicity in this context.

MATERIALS AND METHODS

Study Design and Setting

Forty female Wistar albino rats were housed in groups for 7 to 14 days under standard environmental conditions with free access to food and water. The rats were randomly divided into 5 groups: group 1 (n = 8) was the control group, group 2 (n = 8) received intranasal saline, group 3 (n = 8) received intranasal midazolam, group 4 (n = 8) received intraperitoneal saline, and group 5 received intraperitoneal midazolam (n = 8). Midazolam and saline were administered via intraperitoneal and intranasal routes at doses of 200 μg/kg. Solutions were administered at room temperature in a 1 mL syringe. On the 6th hour after administration, rats were sedated with ketamine (80 mg/kg) and xylazine (5 mg/kg) through intraperitoneal injection. The nasal septal mucosal stripe tissue was removed from the underlying cartilage after sedation.

Pathological Evaluation

Specimens were fixed in 10% neutral buffered formalin for 24 hours at 4°C. All tissues were exposed to ethyl alcohol-graded series' embedded in paraffin blocks. Tissues were sliced in 5 μm sections with a microtome knife. Sections from selected paraffin blocks were placed on poly-L-lysine slides, and deparaffinized at 60°C in the incubator overnight. The sections were then bathed twice in xylene for 30 minutes, rehydrated in absolute alcohol, 95% ethanol, 80% alcohol, and 70% ethanol (3 times) each for 2 minutes, and then washed in distilled water. Antigen retrieval was performed for Ki67 and p53 (10 minutes, citrate buffer pH: 6, 700 Watt microwave oven). The sections were then removed from the microwave, cooled, and washed in distilled water. They were then stained for Ki67 and p53 using an automated method (Ventana Medical Systems, Tucson, AZ). Ki67 and p53 indexes were calculated as the number of positive nuclear immune staining in a total of 1000 cells in randomized areas.

Specimens were also sliced in 5 μm sections and stained with hematoxylin and eosin. All slices were examined by our pathologist blinded to the study under light microscopy to define histopathological changes. The histopathological changes assessed included subepithelial edema, inflammation, cilia loss, and goblet cell distribution on nasal mucosa. To evaluate subepithelial edema, slides were evaluated under magnification of 100, and a score was assigned as follows: 0 (none), 1 (mild), 2 (moderate), or 3 (marked). Hyperplasia of the epidermis, amount of exudate on the epithelial surface, extent of thickening of the dermis, blood and lymph vessel dilation, and infiltration of polymorph nuclear leucocytes (PMNL) and lymphocytes were evaluated to determine the degree of inflammation; these

From the [*]Department of ORL, Dumlupinar University, Kutahya, Turkey; [†]Department of Pathology, Dumlupinar University, Kutahya, Turkey; [‡]Department of Anesthesiology and Reanimation, Dumlupinar University, Kutahya, Turkey; and [§]Department of Biology, Dumlupinar University, Kutahya, Turkey.

Received February 14, 2015.
Accepted for publication May 1, 2015.

Address correspondence and reprint requests to Isa Ozbay, Department of Otolaryngology, Faculty of Medicine, Dumlupinar University, Kutahya, Turkey; E-mail: isaozbay@gmail.com

The abstract of manuscript was submitted to 3rd Congress of European ORL-HNS (7-11 June 2015, Prague, Czech Republic) for oral presentation.
This article was supported by Coordinator of Scientific Research and Project, Dumlupinar University.
The authors report no conflicts of interest.

Copyright © 2015 by Mutaz B. Habal, MD

ISSN: 1049-2275
DOI: 10.1097/SCS.0000000000001965

© 2015 Mutaz B. Habal, MD

Copyright © 2015 Mutaz B. Habal, MD. Unauthorized reproduction of this article is prohibited.

were graded as +, mild inflammation (infiltration of few PMNL and lymphocytes); ++, moderate inflammation (infiltration of some PMNL and lymphocytes); and +++, severe inflammation (severe infiltration of many PMNL and lymphocytes). Cilia loss was evaluated morphologically by light microscopy; it was graded as mild (+), if fewer cilia than normal were noted. If there was a severe loss of cilia, it was graded as moderate (++); and if total loss was observed, it was graded as severe (+++). Visible goblet cell count was enumerated under a magnification of 400×.

Ethical Considerations

All animal procedures were performed in accordance with the European Communities Council Directive of 1986 and approved by the Animal Ethics Committee of Dumlupinar University (2014.04.01).

Statistical Analysis

All data are expressed as means ± standard deviation (SD). Statistical differences in results were determined by Kruskal-Wallis test followed by a Mann-Whitney test. Statistical significance was considered as $P < 0.05$. The Kruskal-Wallis test was used to assess parameter differences according to group, while the Mann-Whitney test was used to evaluate differences.

RESULTS

Ki 67 Staining

The Ki67 value of group 3 (22.75 ± 3.43) was statistically higher than groups 1 (11.25 ± 2.07), 2 (13.75 ± 1.14), and 4 (9.25 ± 1.25, $P < 0.05$) (Table 1, Figs. 1 and 2A–E). On the other hand, there was no statistically significant difference in Ki67 values between group 3 and group 5 (22.88 ± 2.66, $P > 0.05$).

p53 Staining

p53 values of group 3 (12.00 ± 2.60) were higher than group 1 (2.63 ± 1.20), group 2 (7.00 ± 1.72), and group 4 (5.00 ± 1.15); however, these differences were not statistically significant for groups 2 and 4 ($P > 0.05$), but it was statistically significant for group 1 ($P < 0.05$; Table 2, Figs. 3 and 4A–E). There was no statistically significant difference of p53 values between group 3 and group 5 (13.50 ± 1.70, $P > 0.05$).

Inflammation

Comparison of inflammation between group 3 and group 1, group 2, and group 4 revealed a statistically significant difference ($P < 0.01$, $P < 0.05$, $P = 0.01$, respectively, Fig. 5).

Subepithelial Edema

Subepithelial edema assessment between group 3 and the other groups revealed no statistically significant differences ($P > 0.05$, Fig. 6).

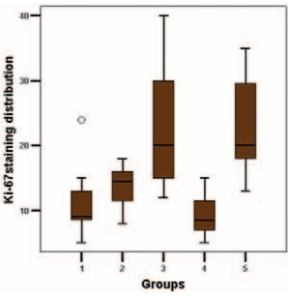

FIGURE 1. Ki67 staining distribution among groups.

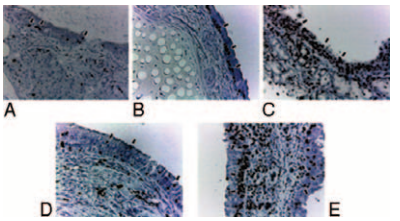

FIGURE 2. (A) Ki67 staining with a 5% proliferation index in the control group. (B) Ki67 staining with a 15% proliferation index in the intranasal saline group. (C) Ki67 staining with a 35% proliferation index in the intranasal midazolam group. (D) Ki67 staining with a 10% proliferation index in the intraperitoneal saline group. (E) Ki67 staining with a 30% proliferation index in the intraperitoneal midazolam group. (×40; arrows indicate cells stained with Ki67).

Cilia Loss

Cilia loss assessment between group 3 and group 1, group 2, and group 4 revealed no statistically significant difference ($P > 0.05$); on the other hand, there was a statistically significant cilia loss in group 5 compared with group 3 ($P < 0.05$, Fig. 7).

Goblet Cell Distribution

Goblet cell loss evaluation between group 3 and group 1 revealed a statistically significant difference ($P < 0.01$); however, there was no statistically significant goblet cell loss between group 3 and group 2, group 4, and group 5 ($P > 0.05$, Figs. 8 and 9A–E).

DISCUSSION

Intranasal administration of drugs has been the focus of much research in recent years. This interest results from the fact that the upper respiratory mucosal has the capability to readily absorb molecules and this makes it a cardinal route for quick and simple drug dispensation.[1] This route of administration seems to be the best choice when rapid drug delivery is crucial, but when drug injection is problematic. Midazolam can be administered by various routes (oral, intramuscular, intravenous, sublingual, rectal, aerosolized buccal, and intranasal) for pediatric sedation induction.[6,11–13] Intranasal midazolam does not cause pain at the administration site, because

TABLE 1. Average Ki-67 Values of All Groups

	Control (G1)		IN Saline (G2)		IN Midazolam (G3)		IP Saline (G4)		IP Midazolam (G5)	
	Mean	SD	Mean	SD	Mean	SD	Mean	SD	Mean	SD
Mean values of Ki-67 staining	11.25	±2.07	13.75	±1.14	22.75	±3.43	9.25	±1.25	22.88	±2.66
P-value compared to IN midazolam	0.008**		0.031*		-		0.003**		0.878	

G = group, IN = intranasal, IP = intraperitoneal.
* $P < 0.05$.
** $P < 0.01$.

© 2015 Mutaz B. Habal, MD

Copyright © 2015 Mutaz B. Habal, MD. Unauthorized reproduction of this article is prohibited.

TABLE 2. Average p53 Values of all Groups

	Control (G1)		IN Saline (G2)		IN Midazolam (G3)		IP Saline (G4)		IP Midazolam (G5)	
	Mean	SD	Mean	SD	Mean	SD	Mean	SD	Mean	SD
Mean value of p53 staining	2.63	±1.20	7.00	±1.72	12.00	±2.60	5.00	±1.15	13.50	±1.70
P-value compared to IN midazolam	0.008*		0.141		-		0.092		0.959	

G = group; IN = intranasal; IP = intraperitoneal.
*$P < 0.05$.

it is a nonparenteral route and is a beneficial and efficient alternative to the oral route in children.[12] Although the intranasal route is viewed positively, the question as to whether intranasal midazolam usage has any side effects on the nasal mucosa is unknown. Information on the cytotoxicity and side effects of midazolam after intranasal administration is lacking in the literature.

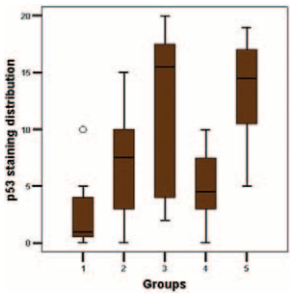

FIGURE 3. P53 staining distribution among groups.

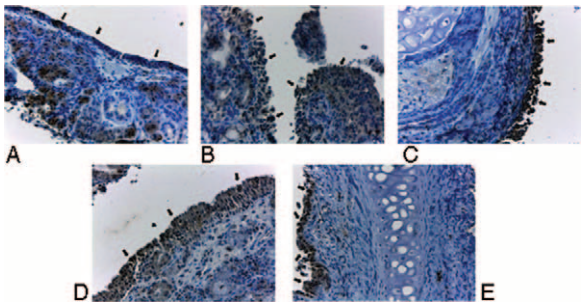

FIGURE 4. (A) P53 staining with a 2% proliferation index in the control group. (B) P53 staining with a 7% proliferation index in the intranasal saline group. (C) P53 staining with an 18% proliferation index in the intranasal midazolam group. (D) P53 staining with an 8% proliferation index in the intraperitoneal saline group. (E) P53 staining with a 15% proliferation index in the intraperitoneal midazolam group. (×40; arrows indicate cells stained with P53).

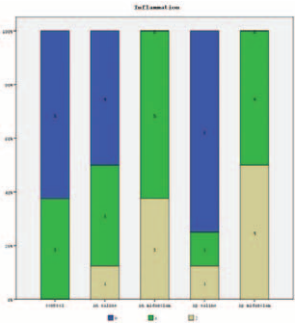

FIGURE 5. Inflammation distribution among groups.

There are a number of studies investigating intranasal midazolam usage under different conditions. For instance, Mekitarian Filho et al[14] investigated impact, outcome, and image quality of intranasal midazolam when used as a single agent for computed tomography (CT) in pediatric patients, and they found that intranasal midazolam is an easy technique for presumable, forceful, and reliable sedation of infants and children for quality CT imaging studies. Humphries and Eiland[15] reviewed the influence, safety, cost, and pharmacokinetics of intranasal midazolam versus rectal diazepam as a treatment for acute seizures for children in prehospital, home, and emergency department settings. Intranasal midazolam was found to be influential and reasonably secure for the treatment of acute seizures in pediatric patients. Therefore, they claimed that intranasal midazolam should be considered as an anticonvulsant agent for community, prehospital, and emergency department use in children when the intravenous route is not favored and rectal access is not available.

Midazolam, dexmedetomidine, buserelin, desmopressin, oxytocin, and calcitonin are drugs that can be administered intranasally. The low permeability of peptides and marked mucosal peptidase activity require an appropriate absorption adjuvant that has low local toxicity to augment systemic absorption. Usually, enzyme

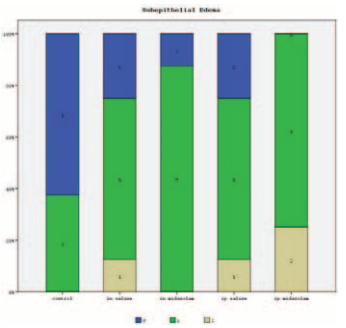

FIGURE 6. Subepithelial edema distribution among groups.

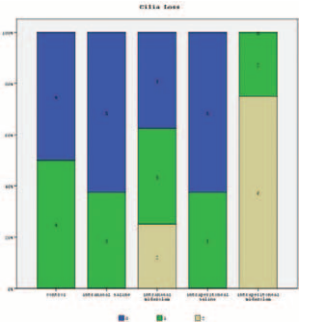

FIGURE 7. Cilia loss distribution among groups.

© 2015 Mutaz B. Habal, MD

Copyright © 2015 Mutaz B. Habal, MD. Unauthorized reproduction of this article is prohibited.

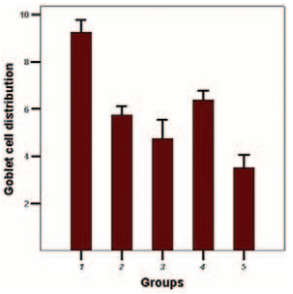

FIGURE 8. Goblet cell distribution among groups.

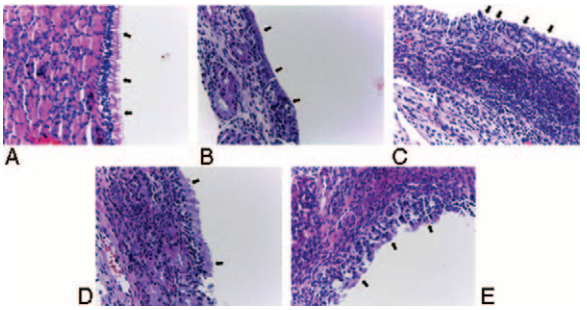

FIGURE 9. (A) Regular arrangement of cilia and goblet cells in the control group (H&E ×40; arrows indicate cilia, circle indicates goblet cells). (B) (+) Goblet and cilia cell loss in the nasal epithelium and inflammation in the subepithelium of the intranasal saline group. (C) (+++) Goblet and cilia cell loss of nasal epithelium and inflammation in the subepithelium of the intranasal midazolam group. (D) (+) Goblet and cilia cell loss of the nasal epithelium and inflammation in the subepithelium of the intraperitoneal saline group. (E) (++) Goblet and cilia cell loss of nasal epithelium and inflammation in the subepithelium of the intraperitoneal midazolam group. (H&E ×40; arrows indicate goblet and cilia cell loss, circle indicates inflammation).

inhibitors and permeation enhancers are required to be coadministered for successful delivery of these biopharmaceuticals. Classes of enhancers have been attributed to specific side effects.[16]

Buserelin is a GnRH analog that is used intranasally. Oghan et al[17] investigated the effects of intranasal buserelin acetate on rabbit nasal mucosa via cytotoxicity compared with saline and demonstrated that nasal buserelin usage had no adverse effect on nasal mucosa of rabbits. Therefore, they suggested that nasal buserelin can be used for all indications with confidence.

Nasal cytotoxicity of another drug was also studied by Hisamatsu et al;[18] they investigated the toxic effects of the human eosinophil granule major basic protein (MBP) on human nasal mucosa in vitro. They found that MBP (5 and 10 μmol/L) significantly inhibited ciliary activity with 4 and 1 hours of exposure, respectively. At these same MBP concentrations, the mucosal surface profiles were altered by 4 hours of exposure, and ciliostasis was 75% to 100% complete by 9 and 6 hours, respectively. In the present study, we also investigated cilia loss after 6 hours from exposure of midazolam, and we found that cilia loss between group 3 and group 1, group 2, and group 4 was not significantly different; on the other hand, there was a statistically significant cilia loss in group 5 compared with group 3. In addition to cilia loss, we also assessed inflammation, subepithelial edema, and goblet cell distribution by histopathology. Suh et al[19] investigated histologic changes after long-term administration of the topical nasal decongestants phenylephrine and oxymetazoline. Administration of phenylephrine and oxymetazoline caused histologic changes, including ciliary loss, epithelial ulceration, inflammatory cell infiltration, and subepithelial edema. In the present study, although group 3 had statistically significant difference in various histopathological parameters compared with group 1, group 2, and group 4, a statistically significant difference was not seen in any of these parameters between group 3 and group 5.

Ki67 antigen expression level is cellular proliferation marker that was also used by Fumic-Dunkic et al.[8] They investigated the correlation between Ki67 expression and clinical stage and its predictive value for the prognosis of laryngeal carcinoma. They found a correlation between carcinoma TNM stage and percentage of Ki67 labeled cells. They also observed an important association between Ki67 reactivity at the time of laryngeal surgery and 2-year clinical disease outcome. In the present study, we also investigated the proliferation of nasal mucosa in rats via Ki67 staining, and we concluded that average of Ki67 values were higher in group 3 compared with group 1, group 2, and group 4.

Mutation or inactivation of the tumor suppressor gene *p53* is often found in malignant neoplasms and is related with early stages of carcinogenesis.[20] Rashad et al[21] investigated the involvement of p53 and Bcl-2 expression in recurrent laryngeal and pharyngeal squamous cell carcinoma, and they claimed that p53 and Bcl-2 mutations appear during the progression of recurrent SCC. In present study, we also investigated apoptosis of nasal mucosa in rats via p53 staining and concluded that p53 values of group 3 were higher than group 1, group 2, and group 4, but statistical significance was only reached with group 1.

CONCLUSIONS

In conclusion, our study, which is the first to investigate the cytotoxic effects of intranasal midazolam on nasal mucosal tissue, found that although intranasal midazolam induces some inflammation, goblet cell loss, nasal mucosa proliferation, and apoptosis, its side effect are not greater than what is seen with systemic usage. Therefore, intranasal midazolam is as safe as systemic administration of midazolam with respect to nasal mucosa. Further studies are needed to confirm our findings.

ACKNOWLEDGMENTS

The authors thank Coordinator of Scientific Research and Project, Dumlupinar University for the support.

REFERENCES

1. Javadzadeh M, Sheibani K, Hashemieh M, et al. Intranasal midazolam compared with intravenous diazepam in patients suffering from acute seizure: a randomized clinical trial. *Iran J Pediatr* 2012;22:1–8
2. Dundee JW, Halliday NJ, Harper KW, et al. Midazolam. A review of its pharmacological properties and therapeutic use. *Drugs* 1984;28:519–543
3. Malinovsky JM, Lejus C, Servin F, et al. Plasma concentrations of midazolam after i.v., nasal or rectal administration in children. *Br J Anaesth* 1993;70:617–620
4. Knoester PD, Jonker DM, Van Der Hoeven RT, et al. Pharmacokinetics and pharmacodynamics of midazolam administered as a concentrated intranasal spray. A study in healthy volunteers. *Br J Clin Pharmacol* 2002;53:501–507
5. Calligaris L, Davide Z, Alessandra M, et al. Concentrated midazolam for intranasal administration: a pilot study. *Pediatr Emerg Care* 2011;27:245–247
6. Chiaretti A, Barone G, Rigante D, et al. Intranasal lidocaine and midazolam for procedural sedation in children. *Arch Dis Child* 2011;96:160–163
7. Lu C, Liu L, Wu X, et al. CD 133 and Ki 67 expression is associated with gastrointestinal stromal tumor prognosis. *Oncol Lett* 2013;6:1289–1294
8. Fumic Dunkic L, Katic V, Janjanin S, et al. Retrospective analysis of Ki-67 antigen expression in paraffin tissue blocks of laryngeal squamous cell carcinoma. *Am J Otolaryngol* 2003;24:106–110
9. Lacroix M, Toillon RA, Leclercq G. p53 and breast cancer, an update. *Endocr Relat Cancer* 2006;13:293–325

© 2015 Mutaz B. Habal, MD

Copyright © 2015 Mutaz B. Habal, MD. Unauthorized reproduction of this article is prohibited.

10. Yamamoto M, Hosoda M, Nakano K, et al. P 53 accumulation is astrong predictor of recurrence in estrogen receptor positive breast cancer patients treated with aromatase inhibitors. *Cancer Sci* 2014;105:81–88
11. Singh R, Kumar N, Vajifdar H. Midazolam as a sole sedative for computed tomography imaging in pediatric patients. *Paediatr Anaesth* 2009;19:899–904
12. Klein EJ, Brown JC, Kobayashi A, et al. A randomized clinical trial comparing oral, aerosolized intranasal, and aerosolized buccal midazolam. *Ann Emerg Med* 2011;58:323–329
13. Dallman JA, Ignelzi MA Jr, Briskie DM. Comparing the safety, efficacy and recovery of intranasal midazolam vs. oral chloral hydrate and promethazine. *Pediatr Dent* 2001;23:424–430
14. Mekitarian Filho E, de Carvalho WB, Gilio AE, et al. Aerosolized intranasal midazolam for safe and effective sedation for quality computed tomography imaging ininfants and children. *J Pediatr* 2013;163:1217–1219
15. Humphries LK, Eiland LS. Treatment of acute seizures: is intranasal midazolam a viable option? *J Pediatr Pharcol Ther* 2013;18:79–87
16. Sayani AP, Chien YW. Systemic delivery of peptides and proteins across absorptive mucosa. *Crit Rev Ther Drug Carr Syst* 1996;13:85–184
17. Oghan F, Apuhan T, Terzi H, et al. Cytotoxic effects of nasal buserelin on nasal mucosal tissue in rabbits. *Eur Arch Otorhinolaryngol* 2012;269:1771–1776
18. Hisamatsu K, Ganbo T, Nakazawa T, et al. Cytotoxicity of human eosinophile granule major basic protein to human nasal sinus mucosa in vitro. *J Allergy Clin Immunol* 1990;86:52–63
19. Suh SH, Chon KM, Min YG, et al. Effects of topical nasal decongestants on histology of rabbit respiratory mucosa in rabbits. *Acta Otolaryngol* 1995;115:664–671
20. Goulart Filho JA, Nonaka CF, da costa Miguel MC, et al. Immunoexpression of cyclooxygenase-2 and p53 in oral squamous cell carcinoma. *Am J Otolaryngol* 2009;30:89–94
21. Rashad UM, Hussein MR, Algizawy SM. Alterations of p53 and Bcl-2 protein expression in the recurrent laryngeal and pharyngeal squamous cell carcinoma. *Am J Otolaryngol* 2011;32:210–214

Effect of Presurgical Positioning on Skull Shape in Sagittal Suture Synostosis

Marie-Lise C. van Veelen, MD, Hansje H. Bredero, MANP,† Clemens M.F. Dirven, MD, PhD,* and Irene M.J. Mathijssen, MD, PhD†*

Purpose: The aim of the this study was to describe changes in head circumference (HC) and cephalic index (CI) in children with sagittal suture synostosis before surgery, by putting the child to bed in supine position lying on the back of the head.

Materials and Methods: A total of 83 patients were scheduled for minimally invasive spring-assisted correction at age 5 to 6 months. At presentation, parents were advised to place their child in bed lying on the back of their head. Preoperative evaluation involved measurement of HC and CI. Head circumference was measured at 2 time points in 33 patients and the CI at 2 time points in 19 patients.

Results: Head circumference (in SD) decreased from 1.69 to 1.37 and the CI increased from 66 to 69.

Conclusion: Before surgery, positioning patients with sagittal suture synostosis on the back of the head is a feasible and effective way of changing head shape. More research is needed to evaluate the postsurgical effects on the long term.

Key Words: Cephalic index, head circumference, positioning, scaphocephaly

Surgical correction for sagittal suture synostosis is generally accepted for both cosmetic and functional reasons; numerous techniques for this are described. In the last decade, the minimally invasive interventions show good cosmetic results compared with the more extensive procedures, and the scars are significantly reduced.[12,14,18,21,24] In the Dutch Craniofacial Center, minimally invasive spring-mediated correction of scaphocephaly was introduced in 2010. Since then, parents are advised to position their child to lie on the back with the head in the same position when in bed. This position is necessary to prevent counteracting the effect of springs, which would occur when sleeping with the head positioned on one side.

Parents are given detailed instructions during their first visit to our outpatient clinic. They are advised to start this positioning before the insertion of the springs to get the child used to lying in this position, before the scheduled surgery. Over the years we have observed considerable preoperative improvement of head shape.

The current study describes the effects on head circumference (HC) and cephalic index (CI) of positioning the child to lie on the back of the head, before surgery takes place.

METHODS

Between January 2010 and December 2013, 83 patients presented at the outpatient clinic for sagittal synostosis. All patients had synostosis of the sagittal suture, confirmed on preoperative computed tomography. Patients presenting before the age of 6 months were offered a minimally invasive spring-mediated distraction.[24] At their first visit, the parents were clearly shown how to position their child to lie on the back of the head. They were provided with a terry cloth holder in

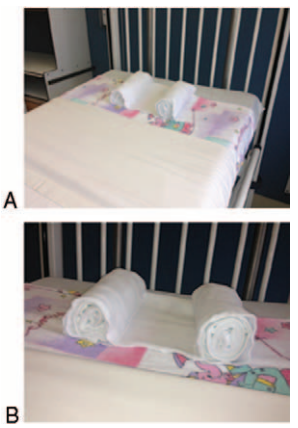

FIGURE 1. A, Terry cloth holder with rolled towels used in the cot. B, Detail of terry cloth holder. It is advised to put the construct under the bottom sheet.

From the *Erasmus University Medical Center Rotterdam, Department of Neurosurgery; and †Erasmus University Medical Center Rotterdam, Department of Plastic and Reconstructive Surgery and Hand Surgery, Rotterdam, The Netherlands.
Received October 7, 2014.
Accepted for publication June 28, 2015.
Address correspondence and reprint requests to Marie-Lise C. van Veelen, MD, Erasmus University Medical Center Rotterdam, Department of Neurosurgery, PO Box 2060, 3000 CB Rotterdam, The Netherlands; E-mail: m.l.c.vanveelen@erasmusmc.nl
The authors report no conflicts of interest.
Clinical trial registration: This study was not subject to the Medical Research Involving Human Subjects Act (WMO), as this study does not involve any form of invasion of the study participant's integrity.
Copyright © 2015 by Mutaz B. Habal, MD
ISSN: 1049-2275
DOI: 10.1097/SCS.0000000000002021

Copyright © 2015 Mutaz B. Habal, MD. Unauthorized reproduction of this article is prohibited.

which 2 tightly rolled towels can be placed to keep the child's head from rotating (Fig. 1A–B). We discussed with the parents the risks of loose objects in the crib and advised to place the construction under the sheet to prevent the child from rolling with its face against the towel or pulling the head holder or the towels over his face.

However, in patients with extensive occipital bulleting this position may create too much flexion, in which case parents are advised to raise the mattress from the shoulders downward, such that the occiput is in a slightly lower position than the thorax.

For all patients, data on HC and CI were collected before surgery, either at presentation or before surgery, or at both time points. Head circumference was measured according to the description by Farkas et al,[7] the CI was calculated according to the description by Haas,[8] taking into account that the direction of largest perimeter and longest diameter is slightly tilted in the scaphocephalic head shape. All measurements were done by the same experienced individual. Intrarater reliability for CI, calculated in 10 patients, was 0.997 ($P = 0.01$), and mean absolute difference was 0.35 (range 0–1.0, SD 0.3). Intrarater reliability for HC, calculated in 10 patients, was 0.993 ($P = 0.01$), and mean absolute difference was 0.08 (range 0.0–0.3, SD 0.1). A large interrater error has been described with measurements of HC by a newly trained individual in newborn infants.[3] However, in a craniofacial setting, a very low inter- and intrarater error has been described for both HC and CI.[25] In this study, only those patients with 2 observations at separate intervals were included for further analysis. Head circumference and CI were compared pairwise using the Wilcoxon signed-rank test.

RESULTS

Head circumference was measured at 2 time points in 33 patients; their mean age at presentation was 0.23 (SD 0.11) years and mean age before surgery was 0.49 (SD 0.07) years. Head circumference (in SD) decreased from 1.69 at presentation to 1.37 before surgery ($P = 0.018$, Z −2.38).

Cephalic index was obtained at 2 time points in 19 patients; their mean age at presentation was 0.25 (SD 0.1) years and mean age before surgery was 0.43 (SD 0.09) years. Mean CI increased from 66 (56–71, SD 3.8) to 69 (62–77, SD 4.0) ($P = 0.004$, Z −2.87). Although the mean difference in CI was 2.8, differences in the individual patient ranged from −3 to as much as +15 (Table 1). Four patients (12%) achieved a CI of 0.75 or higher. Fig. 2A–F are photographs of one of these patients showing correction of the low cranial vertex and elongated skull.

DISCUSSION

This is the first study to describe the effect of positioning of the child on head shape in unoperated sagittal suture synostosis. Sood et al[22] described the effect of preoperative helmeting in 4 patients. However, although CI improved, their study received some criticism because a helmet might constrict growth in the already impaired skull in sagittal suture synostosis.

TABLE 1. Data on Head Circumference and Cephalic Index Measured in 52 Patients

n = 83	At Presentation	Before Surgery
HC: n = 33 pairs		
Age, y (SD)	0.23 (0.11)	0.49 (0.07)
HC (SD)	1.69 (0.98)	1.37 (1.11)
CI: n = 19 pairs		
Age, y (SD)	0.25 (0.1)	0.43 (0.09)
CI (SD, min–max)	66.2 (3.8, 56–71)	69.1 (4.1, 62–77)

CI, cephalic index; HC, head circumference; max, maximum; min, minimum; SD, standard deviation.
HC is given in SD. This results in a mean HC with a SD.

FIGURE 2. A–C, Anteroposterior and lateral photographs of the child at presentation. D–F, Photograph of the same child before surgery. It is advised to put the construct under the bottom sheet.

In the current study, the effect on HC is small but significant, showing that HC decreases with increasing rotundity of the skull and elevation of the vertex. This is an interesting finding because it illustrates that the interpretation of changes in HC and CI with respect to skull growth and volume requires consideration of the shape of the head. For example, in normal Japanese male students a lower HC is associated with a higher CI.[10] A postoperative study by Leikola et al[13] failed to show a relationship between volume and CI, probably because surgery itself introduces confounding factors such as initial enlargement and early closure of the coronal suture.

In our study, the effect on CI is also small but significant. Preoperative CI seems to be an important predictor of postoperative CI (Frontobiparietal remodeling with or without a widening bridge for sagittal synostosis: comparison of 2 cohorts for esthetic and functional outcome. M.L.C. van Veelen, D. Mihajlović, R. Dammers. Accepted for publication). This may imply that preoperative positioning further improves the postoperative result with respect to CI and occipital bulleting.

A drawback of this report is that we did not systematically monitor to what extent positioning on the back of the head was achieved. Children start rolling over from the age of 3 months which makes it difficult to keep children in supine position. However, most parents were highly motivated to comply. Difficulty in sustaining this position was mainly reported with older age, around 9 months, of the child. Incidentally, extensive reflux would prohibit this position.

Supine sleeping, following the "back to sleep" policy, has been shown to cause a mild and transient delay in motor development.[6] Keeping the head in the midline might add to this delay. However, one might as well speculate the opposite. The occipital protuberance forces the head in lateral position and hinders rotation of the head in young scaphocephalic children. Addressing the occipital protuberance may help them to achieve the first developmental milestones more easily.

The use of a head holder may increase the risk of Sudden Infant Death Syndrome (SIDS). Systematical analysis would be necessary

© 2015 Mutaz B. Habal, MD

Copyright © 2015 Mutaz B. Habal, MD. Unauthorized reproduction of this article is prohibited.

to assess the actual risk. Studies on SIDS do report an increased risk with soft bedding, loose objects in the crib, and bumper pads with ties.[5,15,23] The head holder is firmly filled with rolled towels and is not soft. We advise to place the construction under the sheets to prevent the head holder or the towels from changing position and getting draped over the face. We discuss the risk of using this head holder with the parents and advise not to use it in case of reflux, fever, or vomiting.

The endoscopic strip craniectomy, recommended at the age of 3 months, followed by molding helmet is gaining popularity.[19] The helmet remains a point of concern, with respect to volume of the skull, cost, and patient burden.[4] This study shows that rigorous position on the back is effective and might be helpful as alternative to the helmet, as was recently reported.[16,18]

The observation of improved skull shape after positioning on the back raises the question whether in patients who achieve a normal CI surgery is still indicated. However, surgery not only aims at correcting skull shape, but also aims at achieving a normal cranial volume to allow normal brain development. Cognitive development has been shown to be influenced by surgery. Both timing and extend of surgery are important. Surgery performed before the age of 6 months is associated with a better neurodevelopmental outcome than surgery performed between 6 and 12 months or after 12 months.[1,9] Also, a more extensive procedure is associated with a better neurodevelopmental outcome than a (extended) strip craniectomy, especially when the latter is performed before the age of 3 months.[9] Bellew et al[2] showed that not operating results in a deterioration of motor development. Moreover, the risk of raised intracranial pressure in unoperated sagittal suture synostosis is as high as 10% to 80%.[11,17,20] Expansive surgery, therefore, seems essential in the management of sagittal synostosis. The role of positioning is to support such surgery.

CONCLUSION

Preoperative positioning on the back of the head is feasible in most patients with sagittal synostosis and is effective in reducing CI. Head circumference decreases, probably due to decrease of the occipital bullet and elevation of the low vertex. More studies are required to evaluate the long-term effects of this positioning on postoperative results.

REFERENCES

1. Arnaud E, Renier D, Marchac D. Prognosis for mental function in scaphocephaly. *J Neurosurg* 1995;83:476–479
2. Bellew M, Liddington M, Chumas P, et al. Preoperative and postoperative developmental attainment in patients with sagittal synostosis: 5-year follow-up. *J Neurosurg Pediatr* 2011;7:121–126
3. Bhushan V, Paneth N. The reliability of neonatal head circumference measurement. *J Clin Epidemiol* 1991;44:1027–1035
4. Chan JW, Stewart CL, Stalder MW, et al. Endoscope-assisted versus open repair of craniosynostosis: a comparison of perioperative cost and risk. *J Craniofac Surg* 2013;24:170–174
5. Colvin JD, Collie-Akers V, Schunn C, et al. Sleep environment risks for younger and older infants. *Pediatrics* 2014;134:e406–e412
6. Davis BE, Moon RY, Sachs HC, et al. Effects of sleep position on infant motor development. *Pediatrics* 1998;102:1135–1140
7. Farkas LG, Posnick JC, Hreczko TM. Anthropometric growth study of the head. *Cleft Palate Craniofac J* 1992;29:303–308
8. Haas LL. Roentgenological skull measurements and their diagnostic applications. *Am J Roentgenol Radium Ther Nucl Med* 1952;67:197–209
9. Hashim PW, Patel A, Yang JF, et al. The effects of whole-vault cranioplasty versus strip craniectomy on long-term neuropsychological outcomes in sagittal craniosynostosis. *Plast Reconstr Surg* 2014;134: 491–501
10. Hossain MG, Saw A, Alam R, et al. Multiple regression analysis of anthropometric measurements influencing the cephalic index of male Japanese university students. *Singapore Med J* 2013;54:516–520
11. Inagaki T, Kyutoku S, Seno T, et al. The intracranial pressure of the patients with mild form of craniosynostosis. *Childs Nerv Syst* 2007;23:1455–1459
12. Jimenez DF, Barone CM, McGee ME, et al. Endoscopy-assisted wide-vertex craniectomay, barrel stave osteotomies, and postoperative helmet molding therapy in the management of sagittal suture craniosynostosis. *J Neurosurg* 2004;100:407–417
13. Leikola J, Heliövaara KV, Hukki A, et al. Cephalic index correlates poorly with intracranial volume in non-syndromic scaphocephalic patients. *Childs Nerv Syst* 2014;30:2097–2102
14. Massimi L, Di Rocco C. Mini-invasive surgical technique for sagittal craniosynostosis. *Childs Nerv Syst* 2012;28:1341–1345
15. McDonnell E, Moon RY. Infant deaths and injuries associated with wearable blankets, swaddle wraps, and swaddling. *J Pediatr* 2014;164:1152–1156
16. Messing-Junger M, Kunze S, Schmidt C. Is additional helmet therapy really needed in minimal invasive sagittal synostosis surgery? *Childs Nerv Syst* 2014;30:1915
17. Morritt DG, Yeh FJ, Wall SA, et al. Management of isolated sagittal synostosis in the absence of scaphocephaly: a series of eight cases. *Plast Reconstr Surg* 2010;126:572–580
18. Mutchnick IS, Maugans TA. Nonendoscopic, minimally invasive calvarial vault remodeling without postoperative helmeting for sagittal synostosis. *J Neurosurg Pediatr* 2012;9:222–227
19. Proctor MR. Endoscopic cranial suture release for the treatment of craniosynostosis—is it the future? *J Craniofac Surg* 2012;23:225–228
20. Renier D, Sainte-Rose C, Marchac D, et al. Intracranial pressure in craniostenosis. *J Neurosurg* 1982;57:370–377
21. Ridgway EB, Berry-Candelario J, Grondin RT, et al. The management of sagittal synostosis using endoscopic suturectomy and postoperative helmet therapy. *J Neurosurg Pediatr* 2011;7:620–626
22. Sood S, Rozzelle A, Shaqiri B, et al. Effect of molding helmet on head shape in nonsurgically treated sagittal craniosynostosis. *J Neurosurg Pediatr* 2011;7:627–632
23. Thach BT, Rutherford GW Jr, Harris K. Deaths and injuries attributed to infant crib bumper pads. *J Pediatr* 2007;151:271–274
24. van Veelen ML, Mathijssen IM. Spring-assisted correction of sagittal suture synostosis. *Childs Nerv Syst* 2012;28:1347–1351
25. Wilbrand JF, Wilbrand M, Pons-Kuehnemann J, et al. Value and reliability of anthropometric measurements of cranial deformity in early childhood. *J Craniomaxillofac Surg* 2011;39:24–29

Suture Autotransplantation and Dural Stripping for Craniosynostosis: A Long-Term Growth Study in Humans

Maurice Y. Mommaerts, MD, PhD, and Wouter De Vos, MD, MSc†*

From the *European Face Centre, University of Brussels, Brussels, Belgium; and †Southampton University Hospitals NHS Trust, Southampton, UK.

Received May 11, 2014.
Accepted for publication July 9, 2015.

Address correspondence and reprint requests to Prof Maurice Y. Mommaerts, MD, DMD, European Face Centre/Universitair Ziekenhuis Brussel, Laarbeeklaan 101, B-1090 Brussel, Belgium;
E-mail: Maurice.mommaerts@uzbrussel.be

The authors formerly collaborated at the Bruges Cleft and Craniofacial Centre of the General Hospital St. John, Bruges, Belgium (coordinator: M.Y.M.), where this study was conducted.
The authors report no conflict of interest.

Copyright © 2015 by Mutaz B. Habal, MD

ISSN: 1049-2275
DOI: 10.1097/SCS.0000000000002096

© 2015 Mutaz B. Habal, MD

Copyright © 2015 Mutaz B. Habal, MD. Unauthorized reproduction of this article is prohibited.

Objective: Craniosynostosis treatment by suture autotransplantation and dura stripping has proven to be successful in animals. When applied clinically, it may reduce operative morbidity and postoperative growth disturbances known to occur after radical remodeling. It may prevent resynostosis, which is known to occur after simple synostostectomy. It may prevent subcutaneous fluid collections known to occur after synostectomy and dura stripping.
Study design: Four synostostic infants have been treated using this concept and followed up by computerized scans. The distance between markers on each side of the transplanted sutures (6 in total) has been monitored from 1.5 to 7 years.
Results: The transplanted suture areas remained intact, and the sutures remained patent and experienced growth. A fifth patient with similar results was published earlier as a case report.
Conclusions: Suture transplantation and dural stripping should be further studied in future multicenter studies with larger series, comprising syndromic and nonsyndromic synostosis patients.

Until the 1970s, the treatment of craniosynostosis was confined to early extirpation of synostotic sutures, which freed the developing brain for expansion. However, resulting defects were prone to premature reossification, which necessitated repeated interventions.[1]

To prevent deformity after growth completion, radical remodeling of the anterior neurocranium and orbital "bandeau" was adopted as the gold standard of treatment.[2] This approach is not ideal, as it entails a prolonged operative time that confers a substantial risk of transfusion and infection complications.

An alternate strategy is simple craniosynostectomy plus stripping of the osteogenic cambial (periosteal) dura.[3] With this technique, resynostosis does not occur; therefore, cranial growth is unfettered. Unfortunately, subsequent reossification is also severely curtailed, culminating in subcutaneous fluid collection and significant brain vulnerability due to persistent bone defects. By comparison, neurocranial suture autotransplantation (without dura preparation)[4] may offer a substantially better solution for 2 reasons: it addresses the problematic reossification of simple synostectomy by incorporating a bony growth center, and it requires a lesser degree of radical surgical remodeling.

In anticipation of extending this technique to humans in the future, a proof-of-concept study was explored in an animal model. These studies showed that a wholly integrated graft of sutures (in the absence of osteogenic dura) could survive and remain functionally intact for at least the duration of the neurocranial growth spurt.[5–7] The first human trial, coupling suture transplantation with an otherwise classic radical remodeling procedure, involved a child with anterior right-sided plagiocephaly. After stripping of the cambial dura, a healthy, left-sided coronal suture was grafted to the right-sided synostectomy defect. One year later, patency and growth of the grafted suture were confirmed by computed tomography (CT) scanning, and 2 years postoperatively, a satisfactory cosmetic result (good symmetry) was documented.[8]

Based on the success of this initial human trial, 4 additional patients with craniosynostosis were recruited for neurocranial suture autotransplantation. In 2 of these patients, transplantations were performed concurrently at 2 suture sites, yielding a total of 6 sutures for observation. Herein, we report on the long-term growth of these transplanted sutures.

METHODS

This study was approved by the Ethical Committee of General Hospital St. John, Bruges, Belgium (#374), and informed parental consent was obtained for each patient. We obtained Internal Review Board approval to only follow up with 5 patients because CT follow-up in young patients on a large scale is considered inappropriate. Patients with different synostosis types were referred at different ages. Because this was a pilot study and statistical analysis was not the goal, heterogeneity and age differences within the small group helped elucidate the potential of the technique. The first of the series of 5 patients has been described in a previous report.[6]

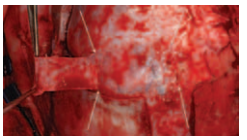

FIGURE 1. Stripping of the cambial (osteogenic) dura at the left coronal synostectomy site (patient 1). The arrows indicate the defect in the cambial dura layer.

Between 2005 and 2009, 4 patients with coronal synostosis underwent neurocranial suture autotransplantation with dural stripping (Fig. 1). During the surgery, grade 5 titanium marker screws of 1-mm diameter (Stryker Leibinger, Freiburg, Germany) were strategically placed with 1 on each side of the transplanted sutures (Fig. 2). The screws, which were originally 4-mm long, were cut to an appropriate length after insertion. In 2 patients (1 and 2), 2 pairs of markers were placed in a single suture, and these pairs were designated as the "medial set" and "lateral set."

Baseline postoperative CT scans, performed within 10 days after surgery, were compared with sequential follow-up CT images (Fig. 3), equating progressive separation of titanium markers with growth of the transplanted sutures. Marker-to-marker increments were measured for each marker pair using OsiriX software (Pixmeo, Geneva, Switzerland). For accuracy, a custom reconstruction slice through both markers was generated through a computer plugin (CMIV CTA Tools, CMIV, Linköping University, Sweden) (Fig. 4). To evaluate the growth of the sutures, the distance between markers on the baseline CT scan was subtracted from the distances measured on subsequent scans, generating a "net" marker-to-marker distance value.

Operative Procedures

Dural stripping is illustrated in Figure 1. The design of the cranial surgery for each of the 4 patients is depicted schematically in

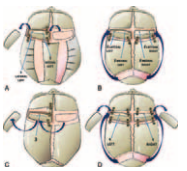

FIGURE 2. Neurocranial suture transplantation topography for each of the 4 patients.

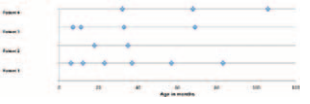

FIGURE 3. Chronology of CT scans for each patient. The first CT is the baseline postoperative scan obtained within 10 days after surgery. CT, computerized tomography.

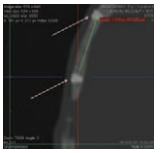

FIGURE 4. Screenshot of the OsiriX image showing the distance between 2 titanium markers (arrows).

© 2015 Mutaz B. Habal, MD

Copyright © 2015 Mutaz B. Habal, MD. Unauthorized reproduction of this article is prohibited.

Figure 2. All transplanted sutures were placed under tensile stress by permanent osteosynthesis.

Patient 1

A male infant with dual synostotic sutures (sagittal and left coronal) underwent surgery at the age of 6 months. The forehead was rotated backward, a bilateral parasagittal ostectomy was performed (from the coronal to lambdoidal sutures), and barrel stave osteotomies in the parietal bone were used to widen the cranium. The left-sided coronal synostosis was then removed, and the subjacent dura was stripped away. A segment of the right-sided coronal suture was harvested and transplanted into the left-sided defect. Two pairs of titanium marker screws, designated as 1 medial and 1 lateral (with 1 representing the patient number), were placed in the transplanted suture.

Patient 2

A 6-month-old male infant was treated for bicoronal synostosis as follows: bilateral coronal synostectomy, bilateral periosteal layer stripping, transplantation of lambdoidal suture segments to the 2 coronal synostectomy defects, and remodeling and advancement of the forehead and orbital bandeau. Two pairs of marker screws were placed in each of the transplanted sutures (designated as 2 medial left, 2 lateral left, 2 medial right, and 2 lateral right).

Patient 3

A female infant with a left-sided coronal synostosis underwent surgery at 6 months of age. Remodeling and advancement of the forehead and supraorbital bandeau were performed on the left side. The left-sided suture was extirpated, and the dura was stripped of its periosteal layer. A segment of right-sided coronal suture was transplanted into the synostectomy defect.

One marker screw was inserted at each side of the transplanted suture (designated as 3).

Patient 4

A female child with bilateral coronal synostosis (genetic, with strong penetrance) underwent surgery when she was 32 months old. No radical remodeling was performed. In consideration of the experience with the 4 preceding patients undergoing suture transplantation and dural stripping (patients 1–3 noted above as well as the child described in a previously published case report),[8] it was agreed that synostectomy, dural stripping, and transplantation of lambdoidal sutures alone offered a chance of growth normalization. One pair of markers was inserted in the suture transplants on each side (designated as 4 left and 4 right).

Statistical Analysis

All software-driven (OsiriX) measurements were obtained by the same individual (WDV) on 2 occasions, 3 weeks apart. Intraobserver error was assessed by determining the intraclass correlation coefficient through two-way mixed effects analysis, using standard software (SPSS Statistics v20, SPSS Inc, Chicago, IL).

RESULTS

Net marker-to-marker distances were obtained for the 9 pairs of markers until the patients reached the following ages: patient 1, 83 months; patient 2, 35 months; patient 3, 69 months; and patient 4, 106 months (Fig. 5). For patient 4, 1 of the markers in the right transplanted suture (4 right marker) became displaced; therefore, a valid measurement at 106 months was not obtained for this marker pair.

Marker separation, representing growth of the transplanted suture, was observed in all sutures except 1 (2 medial right). The fastest rate of growth occurred in patient 1, in whom continued separation was noted for both marker pairs after 6 years of follow-up. The greatest total growth was 27 mm (at 1 medial). The slowest rate of growth was noted in patient 4, who underwent surgery at a relatively later age than the other patients (32 months versus 6 months). For the 3 instances in which 2 pairs of markers were placed in the same transplanted suture, the rate of growth was similar for the pairs in 1 suture (2 medial left and 2 lateral left) but differed by varying degrees for the other sutures (1 medial and 1 lateral, and 2 medial right and 2 lateral right).

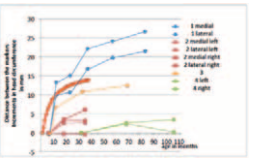

FIGURE 5. Net distance between transplanted suture markers over time for the 9 pairs of markers. No distance value is shown for the 4th right marker pair at 106 months because of displacement of 1 of the markers. Normal cranial growth as exemplified by the increase in head circumference with increasing age in infants and children in the United States (50th percentile: orange). The data were obtained from the US Centers for Disease Control and Prevention (National Center for Health Statistics, Atlanta, GA, USA). The growth increments were very similar for male and female children. Hence, the data for male children only were plotted.

The intraclass correlation coefficient was 1.000 (Table 1). This indicates that there was minimal intraobserver error for the OsiriX marker-to-marker distance measurements.

The nonreconstructed donor synostosectomy sites showed complete suture regrowth as observed on 3D reconstructed and axial CT scans. The transplanted sutures also were fully patent on gross radiographic examination, except the right-sided suture in patient 2 (Fig. 6).

Preoperative and postoperative CT scans as well as other raw data are available from the author upon request.

DISCUSSION

Human neurocranial sutures, whether normal or synostotic, have not been previously targeted for growth monitoring; therefore, no reference dataset is available for comparison. The increase in normal head circumference is depicted in Figure 5. The trend of declining growth measured by this parameter is visually comparable with the trend of growth in the transplanted sutures. The results of the current study show that substantial growth can be achieved at synostotic suture sites by combining the techniques of synostectomy, suture autotransplantation, and cambial dural stripping.

Despite overall successful results from the procedures described herein, there was no apparent growth at 1 of the marker pairs in 1 transplanted suture (the 2 medial right marker set). Possible explanations for this observation include incomplete removal of cambial dura at or near the marker site, allowing for focal ossification and a "zip-lock" phenomenon[9,10] or transplantation of an aberrant suture, programmed to prematurely fuse at that area (Fig. 6). Overall, growth in the transplanted lambda sutures was less pronounced than in the transplanted coronal sutures, possibly indicating an inherent growth difference between these sutural types.

In the single patient with late treatment and no radical remodeling, relatively slow growth of the transplanted sutures was observed. This particular surgery occurred at an age when brain expansion has nearly ceased, which may have contributed to the slow growth. One patient clearly displayed a hereditary form of synostosis (with the mother and 2 other siblings also affected), and none of the patients were syndrome-related. Syndrome-related synostosis may behave differently, because a systematic cause, rather than a local aberration, may be underlying it.

The fusion of sutures can be prevented by altering or blocking dural signaling.[11] One such treatment is transplantation of a

© 2015 Mutaz B. Habal, MD

Copyright © 2015 Mutaz B. Habal, MD. Unauthorized reproduction of this article is prohibited.

TABLE 1. Intraclass Correlation Coefficient Determined by Two-Way Mixed Effects Analysis

		99% Confidence Interval		F Test with True Value 0			
	Intraclass Correlation*	Lower Bound	Upper Bound	Value	Degrees of Freedom 1	Degrees of Freedom 2	Significance Level
Single Measures	1.000†	0.998	1.000	10123.195	5	5	0.000
Average Measures	1.000‡	0.999	1.000	10123.195	5	5	0.000

*Type A intraclass correlation coefficients using an absolute agreement definition.
†The estimator is the same, whether the interaction effect is present or not.
‡This estimate is computed assuming the interaction effect is absent because it is not estimable otherwise.

healthy dura-suture complex to a synostectomy site, whereby the transplanted dura dictates the timing of fusion. Suture-only allografting of synostectomy sites in a rabbit model of congenital synostosis results in allograft synostosis with extensive endosteal hyperostosis.[12] This corroborates with our previous findings in a child with scaphocephaly, which was described in a prior case report.[6] By contrast, the rabbits in Mooney's study[12] that received dura-suture complexes had patent coronal suture transplants and documented suture growth at the last assessment period (59 days after the transplant). The investigators could not definitively state whether the transplanted dura itself provided essential biochemical signals to the suture transplants or synostectomy sites, or if the dura simply functioned as a barrier, preventing biochemical signals required for synostosis from reaching the transplanted suture.

The role of dura in natural (nontransplant) suture fusions has been investigated. In a rat model, isolating the posterior frontal suture from its underlying dura with a silicone sheet extended the initiation of suture fusion from 15 days of age to 30 days of age.[13] Because suture fusion eventually occurred, these results indicate that direct contact with the dura is not always necessary for suture fusion. The authors proposed several possible explanations for eventual suture fusion: a paracrine effect around the silicone sheet barrier, an endocrine signal from a distant source transported to the area through the bloodstream, a direct effect of the silicone sheeting, and/or growth factor release within the surgically created wound.

More recent investigations have suggested that underexpression of transforming growth factor (TGF)-β1 and TGF-β3, as well as overexpression of TGF-β2, promotes calvarial hyperostosis and eventual fusion of bony plates.[14,15] These and other data provide evidence that growth factors emanating from the dura likely play an integral role in the normal process of neurocranial suture fusion. Accordingly, manipulating these factors may have important clinical applications in the treatment of craniosynostosis in the future.

Without underlying synostosis inducing dural tissue, a transplanted suture does not appear to be triggered to fuse prematurely and remains functionally protective. Complete sutural regrowth at suturectomy sites has been documented both in animals[16] and in humans[17]. Hence, extirpation of a normal suture will not leave any anatomical or functional defect at the donor site.

CONCLUSIONS

Synostectomy with cambial dural stripping and suture autotransplantation enabled continued growth at the suture lines, thereby providing growing "helmets" for the brains of 4 young patients with cranial synostosis. These results lead the way for future trials in patients with brachycephaly or plagiocephaly (unrelated to syndromes) to evaluate the effectiveness of transplanted sutures and dural stripping at an early age, without the use of radical remodeling.

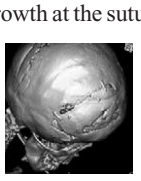

FIGURE 6. The lambda suture transplanted to the right-sided coronal suturectomy defect in patient 2 failed to grow, apparently because of an inherent anatomical or physiological problem in the lambda suture. Consequently, "the zipper was closed."

ACKNOWLEDGMENT

The authors thank Dr Patrick Staels for his kind assistance during the surgical interventions.

REFERENCES

1. Kreiborg S, Pruzansky S. Craniofacial growth in premature craniofacial synostosis. *Scand J Plast Reconstr Surg* 1981;15:171–186
2. Marchac D. Radical forehead remodeling for craniostenosis. *Plast Reconstr Surg* 1978;61:823–835
3. van der Werf AJM. Craniosynostosis. A new operative technique. *Clin Neurol Neurosurg* 1977;80:70–80
4. Stricker M, Raphael B. *Croissance cranio-faciale normale et pathologique*. Reims: Morfos-France, 1993:320–321.
5. Mommaerts MY, Staels P. Coronal suture transplantation to correct fronto-orbital constriction in metopic synostosis. *Int Surg* 1996;81: 210–214
6. Mommaerts MY, Staels PF, Casselman JW. The faith of a coronal suture grafted into midline synostosis inducing dura and deprived from tensile stress. *Cleft Palate Craniofac J* 2001;38:533–537
7. Mommaerts MY, Caemaert J, Dermaut LR, et al. Unicoronal suture autotransplantation in the rabbit. *Childs Nerv Syst* 2003;19:211–216
8. Mommaerts MY, Staels PF. Neurocranial suture autotransplantation and periosteal dura stripping to provide a passive growth site in craniosynostosis: a case report. *J Craniomaxillofac Surg* 2003;31:202–208
9. Mooney MP, Siegel ML, Burrows AM, et al. A rabbit model of human familial, nonsyndromic coronal suture synostosis. 1. Synostotic onset, pathology, and sutural growth patterns. *Childs Nerv Syst* 1998;14: 236–246
10. Reddy K, Hoffman HJ, Armstrong D. Delayed and progressive multiple suture cranio-synostosis. *Neurosurgery* 1990;26:442–448
11. Mommaerts MY. Neurocranial suture autotransplantation in the correction of unicoronal synostosis. PhD Thesis, University of Ghent, 2003c
12. Mooney MP, Burrows AM, Smith TD, et al. Correction of coronal suture synostosis using suture and dura mater autografts in rabbits with familial craniosynostosis. *Cleft Palate Craniofac J* 2001;38:206–225
13. Roth D, Bradley JP, Levine JP, et al. Studies in cranial suture biology: Part II. Role of the dura in cranial suture fusion. *Plast Reconstr Surg* 1996;97:693–699
14. Chong SL, Mitchell R, Moursi A, et al. The effects of TGF-β3 on coronal suture fusion in rabbits. *J Dent Res Abstr* 2002;81: A–462(374)
15. Poisson E, Sciote JJ, Koepsel R, et al. Transforming growth factor-β isoform expression in the perisutural tissues of craniosynostotic rabbits. *Cleft Palate Craniofac J* 2004;41:392–402
16. Mabbutt LW, Kokich VG, Moffett BC, et al. Subtotal neonatal calvariectomy. A radiographiv and histological evaluation of calvarial and sutural redevelopment in rabbits. *J Neurosurg* 1979;51:691–696
17. Joos U. Functional treatment of craniosynostoses during childhood. *Br J Oral Maxillofac Surg* 1998;36:91–98

© 2015 Mutaz B. Habal, MD

Copyright © 2015 Mutaz B. Habal, MD. Unauthorized reproduction of this article is prohibited.